



# Stochastic analysis of biodegradation fronts in one-dimensional heterogeneous porous media

Jack Xin<sup>a</sup> & Dongxiao Zhang<sup>b,\*</sup>

<sup>a</sup>Applied Math Program, University of Arizona, Tucson, AZ 85721, USA

<sup>b</sup>EES-5, MS F665, Los Alamos National Laboratory, Los Alamos, NM 87545, USA

(Received 18 September 1997; revised 23 January 1998; accepted 3 March 1998)

We consider a one-dimensional model biodegradation system consisting of two reaction–advection equations for nutrient and pollutant concentrations and a rate equation for biomass. The hydrodynamic dispersion is ignored. Under an explicit condition on the decay and growth rates of biomass, the system can be approximated by two component models by setting biomass kinetics to equilibrium. We derive closed form solutions for constant speed traveling fronts for the reduced two component models and compare their profiles in homogeneous media. For a spatially random velocity field, we introduce travel time and study statistics of degradation fronts via representations in terms of the travel time probability density function (*pdf*) and the traveling front profiles. The travel time *pdf* does not vary with the nutrient and pollutant concentrations and only depends on the random water velocity. The traveling front profiles are expressed analytically or semi-analytically as functions of the travel time. The problem of nonlinear transport by a random velocity reduces to two subproblems: one being nonlinear transport by a known (unit) velocity, and the other being linear (advective) transport by a random velocity. The approach is illustrated through some examples where the randomness in velocity stems from the spatial variability of porosity. © 1998 Elsevier Science Limited. All rights reserved

*Keywords:* biodegradation fronts, heterogeneities, stochastic analysis.

## 1 INTRODUCTION

Groundwater contamination due to surface spills or subsurface leakage of organic solvents, hydrocarbon fuels, and other organic liquids has recently become a problem of growing concern over the resulting health and environmental problems. Bioremediation is becoming a promising technology for restoring groundwater and soil contaminated with organic pollutants due to its advantage of low cost and *in situ* flexibility. A remedial procedure typically involves the injection of limiting nutrient (electron acceptor, e.g. oxygen and nitrate) into aquifers with pollutants serving as substrate (electron donor) to generate a biologically active zone where indigenous bacteria significantly grow to consume the pollutants.

In recent years, biodegradation has been studied by many researchers through numerical models<sup>1–14</sup>, analytical methods<sup>12,15,16</sup>, and experiments<sup>3,6,7,17</sup>. More recently, stochastic approaches have been used to study the impact of

medium heterogeneity on biodegradation. Ginn *et al.*<sup>5</sup> developed a stochastic–convective reaction model for bio-reaction of a single solute by a single class of microorganisms coupled with dynamic microbial growth. The flow system was represented as an ensemble of purely convective bioreactive stream tubes, each with randomized but spatially constant velocity. Along each stream tube, the transport was governed by two coupled equations, one for substrate and the other for biomass. Then the ensemble averaged solution of the substrate was obtained with the aid of travel time probability density function and the solution for each stream tube. The latter was solved by both numerical and approximate analytical approaches. They found that the method captured the ensemble average large-scale effects of the nonlinear reactions more accurately than in the classical reactive convection–dispersion equation with appropriate scale-dependent dispersion coefficient. Miralles-Wilhelm *et al.*<sup>18</sup> studied the effects of chemical and microbiological variabilities on biodegradation in heterogeneous media. Their analysis was based on a

\*Corresponding author.

system of two coupled equations, one for substrate and the other for nutrient (e.g. oxygen), with time-invariant microbial population.

In the present study, we analyze two reduced two component models which approximate a three component biodegradation system. While the original three equations consist of two reaction–advection equations for substrate and nutrient and one rate equation for biomass, the reduced models consist of two equations for substrate and nutrient. The approximation is valid under an explicit condition on the growth and decay rates of biomass [see eqn (6)]. We discuss closed form traveling fronts in the two component models and compare their profiles in homogeneous media. Then in the case of a spatially random velocity field, we introduce travel time and study the first two statistical moments (ensemble mean and variance) of degradation fronts. These random fronts are written explicitly in terms of the travel time and the closed form homogeneous traveling front profiles. The explicit analytical forms of solutions allow us to examine the effects of randomness on the ensemble averaged front profiles, and to evaluate various physical quantities such as the concentration profiles, the total mass removal and the removal rate. Our study is closely related to the reactive stochastic stream tube approach of Ginn *et al.*<sup>5</sup> in that only advection is considered in both studies. However, our study differs from the latter in the following aspects: (1) the reduced model equations are different; (2) the traveling wave solutions are given analytically or semi-analytically in our study; and (3) not only the expected values of the concentration profiles but also the associated uncertainties are computed in our study.

### 1.1 The basic model

Let us consider the three equation model system of bioremediation as in MacQuarrie *et al.*<sup>9</sup>, Odencrantz *et al.*<sup>11</sup>, and Oya and Valocchi<sup>12</sup>:

$$R_f S_t = DS_{xx} - vS_x - \frac{kmAS}{(K_A + A)(K_S + S)}, \quad (1)$$

$$A_t = DA_{xx} - vA_x - \gamma \frac{kmAS}{(K_A + A)(K_S + S)}, \quad (2)$$

$$m_t = -b(m - m_0) + Y \frac{kmAS}{(K_A + A)(K_S + S)}, \quad (3)$$

where  $S$  = the substrate concentration [ $M_S/L^3$ ];  $A$  = the nutrient (i.e. electron acceptor) concentration [ $M_A/L^3$ ];  $m$  = the microbial biomass concentration [ $M_m/L^3$ ] on a pore volume basis;  $R_f > 1$  = the retardation factor;  $D$  = the hydrodynamic dispersion coefficient [ $L^2/T$ ];  $v$  = the pore water velocity [ $L/T$ ];  $k$  = the maximum rate of substrate utilization [ $M_S M_m^{-1} T^{-1}$ ];  $K_A$  and  $K_S$  = the half-saturation constants of nutrient  $A$  [ $M_A/L^3$ ] and substrate  $S$  [ $M_S/L^3$ ];  $b$  and  $Y$  = the decay [ $T^{-1}$ ] and yield [ $M_m/M_S$ ] constants of biomass  $m$ ;  $m_0$  = the natural biomass population;  $\gamma$  = the stoichiometric constant for nutrient consumption by substrate [ $M_A/M_S$ ].

The product form of nonlinearity in eqns (1)–(3) is called Monod kinetics. There are a few important simplifying assumptions in the model. (1) The substrate is assumed to undergo linear equilibrium sorption and desorption via the retardation factor  $R_f$ , implying that the sorbed pollutants are not directly available as substrate for microbial degradation; (2) the electron acceptor is assumed to be nonsorbing, and this is an appropriate assumption for oxygen and nitrate which are involved in many realistic situations; and (3) all microorganisms responsible for biodegradation are assumed to be attached to the solid phase. From now on, we shall set  $k = 1$ .

We are interested in the initial value problem with bounded nonnegative initial data such that:  $(S, A, m)(0, x) \rightarrow (S^+, 0, m_0), x \rightarrow +\infty$ , and  $(S, A, m)(0, x) \rightarrow (0, A_-, m_0), x \rightarrow -\infty$ , representing the input of nutrient concentration  $A_-$  from the upstream boundary into a medium with pollutant concentration  $S^+$  and biomass  $m_0$ .

Although the linear part of eqns (1)–(3) is hyperbolic with three distinct speeds, the three components evolve together as fronts moving from upstream to downstream due to the reaction terms as long as  $R_f > 1$ . Murray and Xin proved<sup>15</sup> that if  $R_f > 1$  and  $D \geq 0$ , the system of eqns (1)–(3) always admits a traveling wave solution  $(S(x - c_0 t), A(x - c_0 t), m(x - c_0 t), c_0)$  (where  $c_0$  is the traveling wave velocity), satisfying the above boundary conditions at spatial infinities. Moreover, the pollutant profile is decreasing in  $x$ , the nutrient profile is increasing in  $x$ , and the biomass profile has the pulse shape. The front speed is explicit:

$$c_0 = \frac{v(A_- + S^+)}{A_- + R_f S^+}, \quad (4)$$

and the biomass profile has an explicit upper bound:

$$m_0 + Y \frac{(R_f - 1)A_- S^+}{A_- + S^+}. \quad (5)$$

In general, however, front solutions can be moving at constant speeds or time dependent speeds (oscillatory), depending on the parameter regimes. The role of dispersion  $D$  is quite standard. It helps stabilize the fronts and also widens the front width. Because of this, we shall ignore dispersion  $D$  in this paper. The other reason is that closed form formulae are hard to come by for fronts with nonzero  $D$ . So our results in this paper deal only with pure advection.

Xin and Hyman<sup>16</sup> showed that if:

$$\frac{Y}{b} < \left(1 + \frac{K_A}{A_-}\right) \left(1 + \frac{K_S}{S^+}\right), \quad (6)$$

the long time behavior of the three component system of eqns (1)–(3) can be approximated by that of the two equation system obtained by setting the biomass kinetics to equilibrium. It is seen from eqn (6) that the condition may be satisfied if the substrate and nutrient concentrations  $A_-$  and  $S^+$  are low compared to the half-saturation constants  $K_A$  and  $K_S$ , e.g. in a relatively dilute system, and/or if the yield constant  $kY$  is smaller than the decay constant  $b$

(note  $k = 1$  in this study). The reduced two component system is:

$$R_f S_t = -v S_x - \mathfrak{R}, \quad (7)$$

$$A_t = -v A_x - \gamma \mathfrak{R}, \quad (8)$$

with  $m$  expressed as:

$$m = b m_0 \left[ b - \frac{YAS}{(K_A + A)(K_S + S)} \right]^{-1}, \quad (9)$$

and

$$\mathfrak{R} = \frac{m_0 AS}{K_A K_S + K_A S + K_S A + (1 - b^{-1} Y) AS}. \quad (10)$$

In other words, the reduction is obtained by setting the right hand side of eqn (3) to zero, as  $m$  will eventually approach the relaxed equilibrium state given by eqn (9).

In the nutrient-deficient regime ( $K_A$  and  $K_S$  being large compared with  $(A, S)$ ), we further simplify eqns (7) and (8) to:

$$R_f S_t + v S_x = -\frac{m_0}{K_A K_S} AS, \quad (11)$$

$$A_t + v A_x = -\frac{\gamma m_0}{K_A K_S} AS. \quad (12)$$

In the nutrient-sufficient regime,  $\mathfrak{R}$  tends to  $m_0' = m_0(1 - b^{-1} Y)^{-1}$  times the Heaviside function  $H(AS)$ , where  $H = 1$  if  $AS > 0$ ,  $H = 0$  if  $AS = 0$ . The system becomes:

$$R_f S_t = -v S_x - m_0' H(AS), \quad (13)$$

$$A_t = -v A_x - m_0' H(AS), \quad (14)$$

which has been integrated explicitly in Ref. <sup>12</sup> to find oscillatory traveling front solutions of the form  $(S, A) = (S, A)(x - c_0 t, t)$ , periodic in  $t$ .

## 1.2 The stochastic model

Now let us extend the basic model to the context of stochastic water velocity situation:

$$R_f S_t = -v(x) S_x - \frac{kmAS}{(K_A + A)(K_S + S)} \quad (15)$$

$$A_t = -v(x) A_x - \frac{kmAS}{(K_A + A)(K_S + S)} \quad (16)$$

$$m_t = -b(m - m_0) + Y \frac{kmAS}{(K_A + A)(K_S + S)} \quad (17)$$

where  $v(x) = q/n(x)$  is the water seepage velocity,  $n(x) = n(x, \omega)$  is the random porosity function (defined over scale  $\omega$ ), and  $q$  is the water flux. Here we consider divergence-free flow,  $q_x = 0$  such that  $q$  is spatially constant in one dimension. However,  $q$  can be a random constant (e.g. due to a random boundary condition). Again, we assume the initial biomass  $m_0$  to be constant as in Ginn *et al.* <sup>5</sup> and let  $k = 1$ .

With the travel time:

$$T = T(x, x_0) = \int_{x_0}^x dx/v(x), \quad (18)$$

we put eqns (15)–(17) into a constant coefficient system:

$$R_f S_t + S_T = -\frac{mAS}{(K_A + A)(K_S + S)}, \quad (19)$$

$$A_t + A_T = -\gamma \frac{mAS}{(K_A + A)(K_S + S)}, \quad (20)$$

$$m_t = -b(m - m_0) + Y \frac{mAS}{(K_A + A)(K_S + S)}. \quad (21)$$

In the rest of this paper, we will perform statistical studies of these random fronts for the nutrient-deficient model and the general two component model.

## 2 RANDOM TRAVELING FRONTS

### 2.1 The nutrient-deficient model

The condition of eqn (6):  $Y/b < (1 + K_A/A_-)(1 + K_S/S^+)$ , which can be achieved when  $K_A$  and  $K_S$  are large compared with  $(A^-, S^+)$ , results in the following simplified system of equations:

$$R_f S_t + S_T = -\frac{m_0}{K_A K_S} AS, \quad (22)$$

$$A_t + A_T = -\frac{\gamma m_0}{K_A K_S} AS, \quad (23)$$

which is the system under study in this section. In this case, over long time  $m = m_0$ . Consider the change of variables for eqns (22) and (23):

$$u = \gamma R_f S - A, \quad w = \gamma S - A, \quad (24)$$

or:

$$A = (R_f - 1)^{-1}(u - R_f w), \quad S = \gamma^{-1}(R_f - 1)^{-1}(u - w). \quad (25)$$

hen  $(u, w)$  satisfies the system in conservation form:

$$u_t + w_x = 0, \quad (26)$$

$$w_t + ((1 + R_f^{-1})w - R_f^{-1}u)_x = \tilde{\gamma}(u - w)(u - R_f w), \quad (27)$$

where  $\tilde{\gamma} = R_f^{-1}(R_f - 1)^{-1}m_0(K_A K_S)^{-1}$ . The explicit traveling front solutions of the form  $(u_0, w_0)(\xi)$ ,  $\xi = T - c_0 t$ , are [see Appendix A]:

$$c_0 = \frac{\gamma S^+ + A_-}{\gamma R_f S^+ + A_-}, \quad (28)$$

$$u_0 = \frac{1}{c_0} w_0 + \left( -1 + \frac{1}{c_0} \right) A_-, \quad (29)$$

$$w_0 = \frac{\gamma S^+ - A_-}{2} + \frac{\gamma S^+ + A_-}{2} \tanh \left( \frac{1}{2} R_f (\gamma R_f S^+ + A_-) \tilde{\gamma} \xi \right). \quad (30)$$

Such solutions are unique up to a constant translate in  $\xi$ . In the original variables  $(S, A)$ , we have, in view of eqn (25), the explicit expression of random traveling fronts:

$$A(T, t) = \frac{A_-}{2} \left[ 1 - \tanh \left( \frac{m_0}{K_A K_S} \frac{A_- + \gamma R_f S^+}{2(R_f - 1)} (T - c_0 t) \right) \right], \quad (31)$$

and

$$S(T, t) = \frac{S^+}{2} \left[ 1 + \tanh \left( \frac{m_0}{K_A K_S} \frac{A_- + \gamma R_f S^+}{2(R_f - 1)} (T - c_0 t) \right) \right], \quad (32)$$

where  $c_0$  is given in eqn (28) and the random travel time  $T$  in eqn (18).

## 2.2 The general two component model

Let us consider the more general model without restrictive assumptions about  $K_A$  and  $K_S$  but still under biomass equilibrium conditions:

$$R_f S_t + S_T = - \frac{m_0}{K_A K_S} AS/F(A, S), \quad (33)$$

$$A_t + A_T = - \gamma \frac{m_0}{K_A K_S} AS/F(A, S), \quad (34)$$

$$m = bm_0 \left[ b - \frac{YAS}{(K_A + A)(K_S + S)} \right]^{-1}, \quad (35)$$

where:

$$F(A, S) = 1 + S/K_S + A/K_A + (1 - b^{-1}Y)AS/(K_A K_S). \quad (36)$$

Making the same change of variables to  $(u, w)$  as in eqns (24) and (25), and following the same procedure as before, we have the same expressions as eqns (28) and (29). The only change is that eqn (30) is modified to:

$$\frac{dw_0}{d\xi} = - \frac{\tilde{\gamma} R_f (\gamma R_f S^+ + A_-)}{(\gamma S^+ + A_-)} (w_0 - S^+) (w_0 + A_-) / G(w_0), \quad (37)$$

where  $G = G(w)$  is simply  $F(A, S)$  with  $A$  and  $S$  written as functions of  $w$  using eqns (25) and (29).  $G(w)$  is a positive quadratic function of  $w$ , and is equal to:

$$\begin{aligned} G(w) &= 1 + (\gamma K_S (R_f - 1))^{-1} (c_0^{-1} - 1) (w + A_-) \\ &+ (R_f - 1)^{-1} K_A^{-1} (c_0^{-1} - R_f) \left( w + \frac{1 - c_0}{1 - R_f c_0} A_- \right) \\ &+ (1 - b^{-1}Y) \frac{(c_0^{-1} - 1)(c_0^{-1} - R_f)}{K_A K_S \gamma (R_f - 1)^2} (w + A_-) \\ &\times \left( w + \frac{1 - c_0}{1 - R_f c_0} A_- \right) \end{aligned}$$

which simplifies using the wave speed formula for  $c_0$  to:

$$\begin{aligned} G(w) &= 1 + \frac{S^+ (w + A_-)}{K_S (\gamma S^+ + A_-)} - \frac{A_- (w - \gamma S^+)}{K_A (\gamma S^+ + A_-)} \\ &- (1 - b^{-1}Y) \frac{S^+ A_- (w + A_-) (w - \gamma S^+)}{K_S K_A (\gamma S^+ + A_-)^2}. \quad (38) \end{aligned}$$

The solutions of  $A$  and  $S$  are given by eqn (25) as  $w_0$  is solved from eqn (37), see Appendix B.

## 3 STATISTICAL ANALYSIS OF RANDOM FRONTS

### 3.1 General formalism

Because  $T$  is a random variable, so are nutrient concentration  $A(x, t)$ , substrate concentration  $S(x, t)$  and biomass concentration  $m(x, t)$ . They may be estimated with their ensemble means (expected values):

$$\langle A(x, t) \rangle = \int_0^\infty A(T, t) f(T; x, x_0) dT, \quad (39)$$

$$\langle S(x, t) \rangle = \int_0^\infty S(T, t) f(T; x, x_0) dT \quad (40)$$

$$\langle m(x, t) \rangle = \int_0^\infty m(T, t) f(T; x, x_0) dT \quad (41)$$

where  $A(T, t)$ ,  $S(T, t)$  and  $m(T, t)$  are given earlier, and  $f(T; x, x_0)$  is the probability density function (*pdf*) of the travel time  $T(x, x_0)$  of a particle from  $x_0$  to  $x$ . Note that after averaging, the dependence on  $(x, t)$  in eqns (39), (40) and (41) is not of the form  $x - ct$ . Hence strictly speaking,  $\langle A \rangle$ ,  $\langle S \rangle$ , and  $\langle m \rangle$  are not traveling waves. However, they do behave like traveling waves in the sense that they move at constant speeds to leading order in time. The evaluation of the expected concentrations reduces to that of travel time *pdf*, which only depends on the water velocity and does not vary with the nutrient or substrate wave front speed. The uncertainty associated with the estimation can be evaluated with the variances:

$$\begin{aligned} \sigma_A^2(x, t) &= \langle A^2(x, t) \rangle - \langle A(x, t) \rangle^2 = \int_0^\infty A^2(T, t) f(T; x, x_0) \\ &\times dT - \langle A(x, t) \rangle^2, \quad (42) \end{aligned}$$

$$\sigma_S^2(x, t) = \int_0^\infty S^2(T, t) f(T; x, x_0) dT - \langle S(x, t) \rangle^2, \quad (43)$$

$$\sigma_m^2(x, t) = \int_0^\infty m^2(T, t) f(T; x, x_0) dT - \langle m(x, t) \rangle^2. \quad (44)$$

As mentioned earlier, the randomness in  $v(x)$  may stem from  $q$  and/or  $n(x)$ . In the case of one-dimensional, steady-state flow,  $q$  can be either a deterministic or random constant. The latter represents the ensemble of 1-D columns of different  $q$  or a single column with random boundary conditions. In this case the travel time moments can, however, only be given via approximation. In this study, we consider the case that  $q \equiv q_0$  is a specified

constant such that the spatial variability in porosity is the only source of randomness in the velocity  $v(x) = q_0/n(x)$ . The porosity is assumed to be stationary such that its mean  $\langle n \rangle$  is constant and its covariance  $C_n(x, x_1)$  only depends on the relative distance  $r = x - x_1$ . The covariance function  $C_n$  is taken to be exponential:

$$C_n(r) = \sigma_n^2 \exp\left[-\frac{|r|}{\lambda_n}\right] \quad (45)$$

where  $\sigma_n^2$  and  $\lambda_n$  are the variance and correlation scale of porosity, respectively.

In this case, the travel time can be rewritten as:

$$T(x, x_0) = \int_{x_0}^x \frac{n(x')}{q_0} dx'. \quad (46)$$

Hence, its moments are given exactly as:

$$\langle T(x, x_0) \rangle = \frac{\langle n \rangle}{q_0} (x - x_0), \quad (47)$$

$$\begin{aligned} \sigma_T^2(x) &= \frac{1}{q_0^2} \int_{x_0}^x \int_{x_0}^x C_n(x' - x'') dx' dx'' \\ &= \frac{2}{q_0^2} \int_{x_0}^x (x - x') C_n(x' - x_0) dx' \\ &= \frac{2\sigma_n^2}{q_0^2} \left\{ \lambda_n (x - x_0) - \lambda_n^2 \left[ 1 - \exp\left(-\frac{x - x_0}{\lambda_n}\right) \right] \right\}. \end{aligned} \quad (48)$$

It is seen that the travel time variance increases sublinearly with  $(x - x_0)$ .

If the travel time obeys a lognormal distribution, its *pdf* can be described with the first two moments:

$$f(T; x, x_0) = \frac{1}{(2\pi)^{1/2} T \sigma_{\ln(T)}} \exp\left\{-\frac{\{\ln(T) - \langle \ln(T) \rangle\}^2}{2\sigma_{\ln(T)}^2}\right\}, \quad (49)$$

where  $\langle \ln(T) \rangle = -0.5 \ln[\langle T \rangle^2 + \sigma_T^2] + 2 \ln(\langle T \rangle)$  and  $\sigma_{\ln(T)}^2 = \ln[\langle T \rangle^2 + \sigma_T^2] - 2 \ln(\langle T \rangle)$ . Although other forms of travel time *pdfs* are possible, it is found by Zhang and Tchepeli<sup>19</sup> for a similar problem of random Buckley-Leverett displacement that the impact of distributional forms may be neglected. With eqn (49) the means and variances of concentrations in eqns (39)–(44) can be evaluated by numerical integrations, say via Simpson's rule.

Another quantity of interest is the substrate removal in the domain segment from  $x_0$  to  $x_1$ :

$$R(t; x_1, x_0) = \int_{x_0}^{x_1} R_f n(x) [S^+ - S(x, t)] dx, \quad (50)$$

which can be estimated with its expected value:

$$\begin{aligned} \langle R(t; x_1, x_0) \rangle &= \int_{x_0}^{x_1} R_f [\langle n \rangle S^+ - \langle n(x) S(x, t) \rangle] dx \\ &= \int_{x_0}^{x_1} R_f \left[ \langle n \rangle S^+ - \int_0^1 \int_0^\infty n(x) S(T, t) f[n(x); \right. \\ &\quad \left. T(x, x_0)] dn dT \right] dx. \end{aligned} \quad (51)$$

Here  $f[n(x); T(x, x_0)]$  is the joint *pdf* of the porosity  $n$  at  $x$  and the travel time from  $x_0$  to  $x$ . It can easily be shown that the cross covariance between  $n(x)$  and  $T(x, x_0)$  is given as:

$$\langle n'(x) T'(x, x_0) \rangle = \frac{\lambda_n \sigma_n^2}{q_0} \left[ 1 - \exp\left(-\frac{x - x_0}{\lambda_n}\right) \right], \quad (52)$$

where the superscript ' indicates deviation from the mean. With this and eqn (48), we obtain immediately that the correlation function between  $n(x)$  and  $T(x, x_0)$ ,  $\rho_{nT}(x - x_0) = \langle n'(x) T'(x, x_0) \rangle / [\sigma_n \sigma_T(x)] \rightarrow 0$  as  $x - x_0 \rightarrow \infty$ . That is to say,  $n(x)$  and  $T(x, x_0)$  become uncorrelated when the distance  $x - x_0$  is large (relative to  $\lambda_n$ ). Physically speaking, this is so because the influence of  $n(x)$  on  $T(x, x_0)$  becomes smaller and smaller as the distance  $x - x_0$  increases.

Below we evaluate the statistical moments for two specific models.

### 3.2 The nutrient-deficient model

In the case of  $Y/b < (1 + K_A/A^-)(1 + K_S/S^+)$  with  $(K_A, K_S)$  being large compared with  $(A, S)$ ,  $m$  is equal to  $m_0$  over long time. It is seen from eqns (31) and (32) that:

$$\frac{A(x, t)}{A_-} + \frac{S(x, t)}{S^+} = 1. \quad (53)$$

With this, we have:

$$\frac{\langle A(x, t) \rangle}{A_-} + \frac{\langle S(x, t) \rangle}{S^+} = 1, \quad (54)$$

$$\frac{\sigma_A^2(x, t)}{A_-^2} = \frac{\sigma_S^2(x, t)}{S^{+2}}. \quad (55)$$

Hence, it suffices to compute the mean and variance for either  $A$  or  $S$ .

We consider the case of semi-infinite domain where the nutrient concentration is kept constant as  $A_-$  at  $x_0 = 0$  and the substrate concentration remains to be  $S^+$  at  $x = \infty$ . This represents the situation of continuous injection of nutrient from the upstream into a large column with pollutant concentration  $S^+$  and biomass concentration  $m_0$ . In the following examples,  $A_- = 1.0$ ,  $S^+ = 1.0$ ,  $R_f = 1.5$ ,  $\gamma = 2.0$ ,  $K_A K_S = 10.0$  and  $q_0 = 0.3$  unless stated otherwise. Only porosity is assumed to vary spatially with  $\langle n \rangle = 0.3$ ,  $\sigma_n^2 = 0.09$  and  $\lambda_n = 1.0$  (unless stated otherwise). All these parameters are given in a set of arbitrary but consistent units.

Fig. 1 shows the expected (mean) concentrations of nutrient and substrate and the concentration standard deviation at two times and for different variabilities in porosity. The mean concentrations are normalized as  $\langle A \rangle / A_-$  and  $\langle S \rangle / S^+$ , and the concentration standard deviation as  $\sigma_A / A_- = \sigma_S / S^+$ . It is seen that at  $t = 50$ , the nutrient concentration drops from unity rapidly near  $x = 0$  even in the homogeneous case of  $\sigma_n^2 = 0$  while this sudden drop in concentration disappears at  $t = 150$ . The rapid decrease near  $x = 0$  at early time is due to the approximation of continuous injection boundary condition at  $x = 0$  in

our example while the analytical solution of eqns (31) and (32) is derived by assuming the boundary to be at  $x = -\infty$ . The effect of this approximation disappears at later time (at least, at  $t = 150$ ). Then, the nutrient concentration becomes one at the left side of the domain and decreases gradually toward zero while the substrate concentration is zero at the left side and increases gradually to one. It can be seen from eqns (31) and (32) with  $T = (x - x_0)/v$  ( $v$  being a deterministic velocity) that the nutrient and substrate concentration profiles (fronts) retain the same shape through time but travel at the speed  $c_0v$  in the homogeneous case after the boundary effect disappears. The reason for the invariant concentration profiles is that local dispersion  $D$  is neglected. In the presence of spatial variability in porosity, dispersion is induced, resulting in less steep fronts for the expected nutrient and substrate concentrations (Fig. 1(a,b)). In addition, the heterogeneity induced dispersion increases with time. However, it seems that the expected fronts also travel at the constant speed  $c_0\langle v \rangle$ , where  $\langle v \rangle = q_0\langle n \rangle$ . The concentration standard deviation (uncertainty) is largest at or near the center of the front and moves at the same speed as the expected front, and its peak value increases with time. It is also seen that both

the effective dispersion and the concentration uncertainty increase with the variance of porosity. Here the value of  $\sigma_n^2 = 0.25$  may be too large for most real situations and is assumed only for the purpose of illustration.

Fig. 2 investigates the impact of the correlation scale of porosity on the concentration moments. In this case,  $\sigma_n^2 = 0.25$ . It is seen that both the magnitude of dispersion and the concentration standard deviation (uncertainty) increase with the correlation scale.

Figs 3 and 4 look at the sensitivities of various geochemical and biological parameters. In these cases,  $\langle n \rangle = 0.3$ ,  $\sigma_n^2 = 0.09$  and  $\lambda_n = 1.0$ . It is seen that the results are quite sensitive to these parameters. A smaller retardation factor not only makes the concentration fronts move faster but also increases the peak concentration standard deviation (Fig. 3(a,c)). An increase in the stoichiometric constant for nutrient consumption (from  $\gamma = 2$  to 3) renders the expected fronts slightly retarded and enhances the peak standard deviation (Fig. 3(b,d)). A larger initial biomass concentration  $m_0$  gives a steeper expected concentration front and larger uncertainty in estimating the fronts (Fig. 4(a,c)).

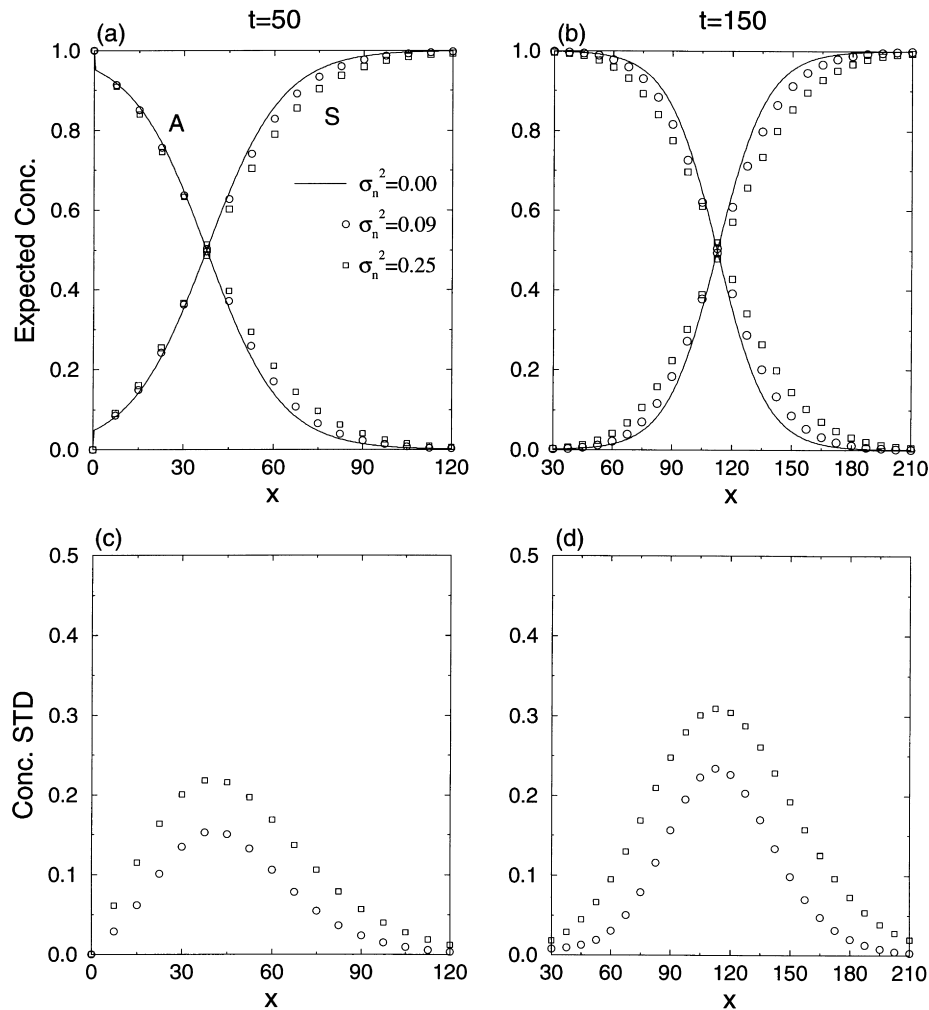


**Fig. 1.** Expected values and standard deviations of nutrient and substrate concentrations for different porosity variances ( $\sigma_n^2 = 0, 0.09$  and  $0.25$ ): (a) and (c)  $t = 50$ ; (b) and (d)  $t = 150$ . (The nutrient-deficient model.)

Comparing the two curves for  $S/S^+$  in Fig. 4(a), the left side is much cleaner (with smaller concentration) with  $m_0 = 0.5$  than with  $m_0 = 0.1$ . This is so because more bacteria are available there in the former case. The larger the product of  $K_A$  and  $K_S$  (half-saturation constants of nutrient and substrate, respectively), the less steep are the concentration fronts and the lower is the peak of concentration standard deviation (Fig. 4(b,d)). Note that  $m_0$  and  $K_A(K_S)$  do not affect the traveling speed of the mean profiles. Since these biological and geochemical parameters significantly impact the concentration prediction and the associated uncertainty, the uncertainty and/or spatial variability in these parameters, if any, should be investigated in future studies.

Now, let us look at the expected substrate removal. It is seen from Fig. 1(b,d) that at time  $t = 150$ ,  $\langle S \rangle \approx 0$  and  $\sigma_S \approx 0$  for small  $x - x_0$  (with  $x_0 = 0$ ). That is, for small distance  $x$ ,  $S$  is primarily controlled by the boundary condition at the left side and is essentially independent of  $n(x)$  at large time. As discussed in the previous section, for large distance it is always true that  $n(x)$  and  $T(x, x_0)$  are uncorrelated.

Therefore, at large time we may approximate the expected substrate removal eqn (51) as:

$$\begin{aligned} \langle R(t; x_1, x_0) \rangle &= R_f \langle n \rangle S^+ \int_{x_0}^{x_1} \left[ 1 - \frac{\langle S(x, t) \rangle}{S^+} \right] dx \\ &= R_f \langle n \rangle S^+ \int_{x_0}^{x_1} \frac{\langle A(x, t) \rangle}{A_-} dx, \end{aligned} \quad (56)$$

which is achieved by letting  $\langle n(x)S(x, t) \rangle \approx \langle n(x) \rangle \langle S(x, t) \rangle$ .

Fig. 5(a,c) shows the expected substrate removal and its rate as a function of time for one homogeneous and two heterogeneous cases. Here we choose a very large  $x_1$  to mimic the situation of from 0 to  $\infty$ . For the homogeneous case ( $\sigma_n^2 = 0$ ), the total removal increases almost linearly at large times. This is clear by looking at the removal rate, which increases with time for short times and approaches a constant quickly (Fig. 5(c)). The time varying removal rate at early time is due to the effect of boundary condition as discussed earlier for the expected concentration profiles. With eqns (31) and (56), it can be shown for the homogeneous case that  $d\langle R \rangle / dt = S^+ \langle n \rangle R_f c_0 \langle v \rangle$ . In this case  $d\langle R \rangle / dt = 0.3375$ . It is also seen that the removal rates

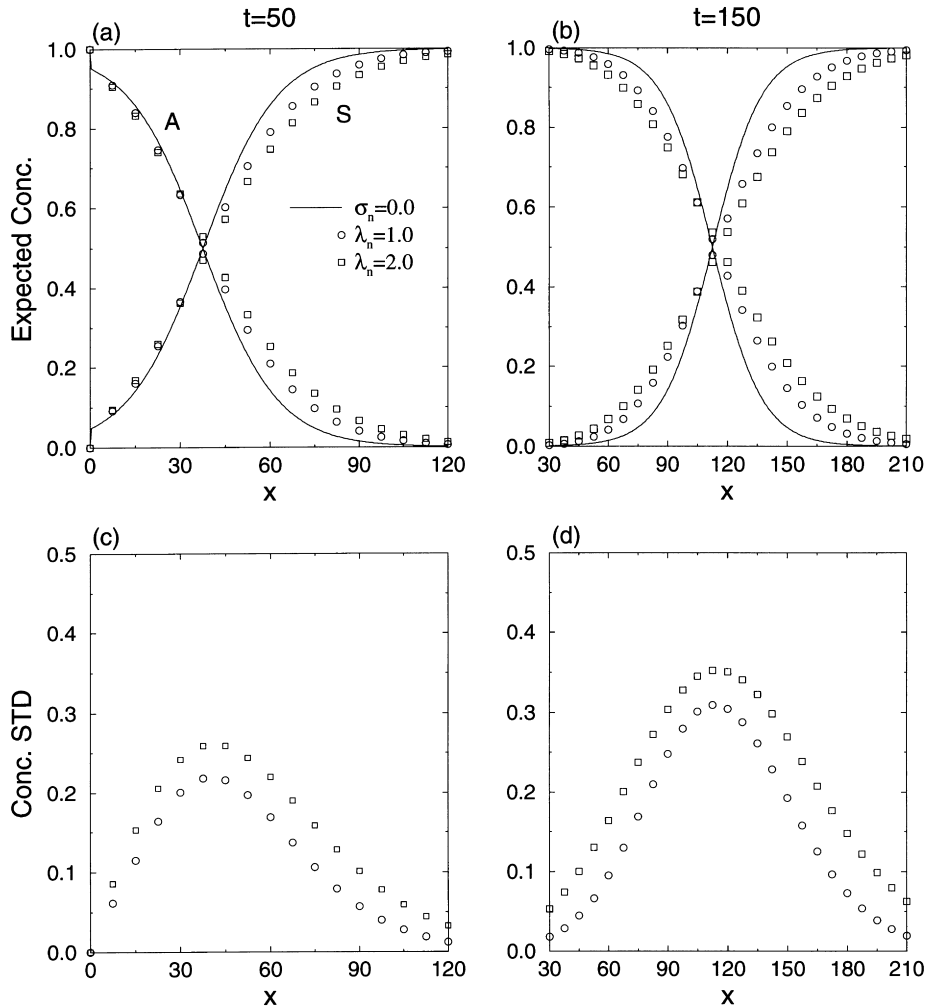


**Fig. 2.** Expected values and standard deviations of nutrient and substrate concentrations for different integral scales of porosity ( $\lambda_n = 1.0$  and 2.0): (a) and (c)  $t = 50$ ; (b) and (d)  $t = 150$ . (The nutrient-deficient model.)

converge to the same value in the heterogeneous cases (Fig. 5(c)). The transient portion of the removal rates are an artifact of the assumption that traveling waves form instantaneously at  $t = 0$ . This, in turn, implies that the observation from Fig. 5(a) that the total substrate removal increases slightly with the magnitude of heterogeneity may also be an artifact due to this assumption. The total substrate removal cannot be assessed accurately with the present (analytical) model because the model behaviors at early travel time before forming traveling waves are not available. However, it may be concluded that medium heterogeneity has no impact on the overall substrate removal rate at later times.

Fig. 5(b,d) shows the effects of biological and geochemical parameters on the substrate removal. In the base case,  $\sigma_n^2 = 0.09$ ,  $\lambda_n = 1.0$ ,  $R_f = 1.5$ ,  $\gamma = 2$ ,  $A_- = 1.0$ ,  $S^+ = 1.0$  and  $m_0 = 0.1$ . In each case, only one parameter is varied as specified in the legend. It is seen that the removal rate decreases significantly as the retardation factor  $R_f$  is reduced from 1.5 to 1.1. This is seemingly counter-intuitive. Based on Fig. 3(a), the clean area with low substrate

concentration is larger when  $R_f = 1.1$  than when  $R_f = 1.5$ , thus the removed substrate mass seems to be larger in the former. However, this only considers aqueous phase mass removal. The sorbed substrate is not directly available for biodegradation. But due to the equilibrium assumption for substrate adsorption, the substrate concentration in the sorbed phase decreases proportionally as the aqueous phase concentration is reduced. The proportionality is  $R_f - 1$ . When the substrate does not sorb onto the solid phase such that  $R_f = 1$ , the removal rate is minimum and is entirely due to clean water flushing. The removal rate is reduced when the stoichiometric constant for nutrient consumption by substrate increases from 2 to 3. This is so because to remove the same amount of substrate more nutrient is needed when  $\gamma$  is larger. In the model that nutrient is a limiting factor, the larger is  $\gamma$ , the smaller is the substrate removal rate. In this nutrient-deficient model, the biomass does not affect the total removal and the removal rate at late times although it impacts the nutrient and substrate concentration profiles (Fig. 4(a,c)). From eqn (31), it is apparent that increasing

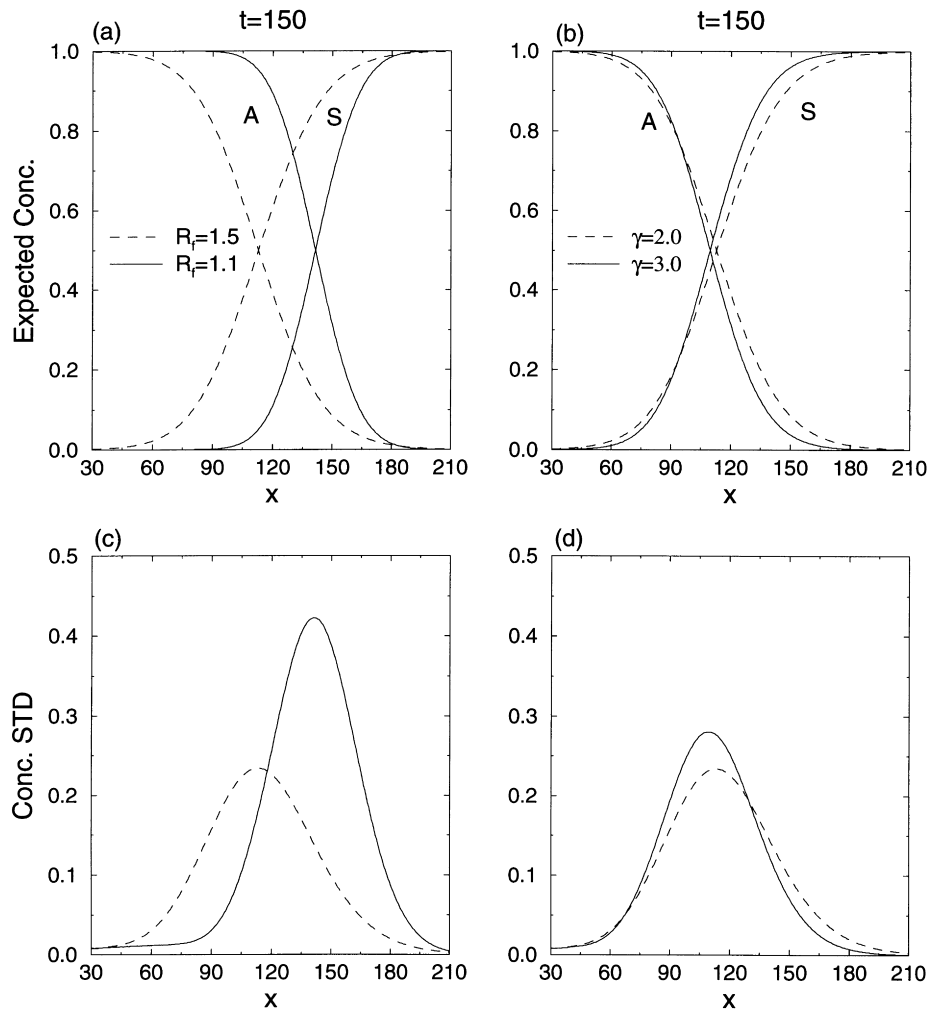


**Fig. 3.** Expected values and standard deviations of nutrient and substrate concentrations at  $t = 150$  for different geochemical and biological parameters: (a) and (c)  $R_f = 1.5$  and  $1.1$ ; (b) and (d)  $\gamma = 2.0$  and  $3.0$ . (The nutrient-deficient model.)

$K_A K_S$  by a factor would have had the same effects as reducing  $m_0$  by the same factor.

In the above, the substrate removal is produced by both biodegradation and clean water flushing from upstream to downstream. The contribution from the latter mechanism is  $S^+ \langle n \rangle v t$ . Hence at large time the biodegradation rate is:

$$\frac{d\langle R_b \rangle}{dt} = S^+ \langle n \rangle v (R_f c_0 - 1) = S^+ A_- \langle n \rangle v \frac{R_f - 1}{\gamma R_f S^+ + A_-} \quad (57)$$

The homogeneous counterpart of eqn (57) has been obtained recently by Oya and Valocchi<sup>12</sup>. It is seen from eqn (57) that the biodegradation rate increases with the mean flux  $\langle n \rangle v$ , the retardation factor  $R_f$ , the initial substrate concentration  $S^+$  and the nutrient concentration  $A_-$ , and decreases with the stoichiometric constant  $\gamma$ . It is also seen that the biodegradation rate does not depend on the initial biomass concentration and the microbial kinetic parameters.

### 3.3 The general two component model

The nutrient and substrate concentrations  $A$  and  $S$  are given as:

$$A(T, t) = (R_f - 1)^{-1} (u_0 - R_f w_0), \quad (58)$$

$$S(T, t) = \gamma^{-1} (R_f - 1)^{-1} (u_0 - w_0), \quad (59)$$

where  $(c_0, u_0)$  is given by eqns (28) and (29), and  $w_0$  is governed by eqn (37). One may solve for  $w_0$  based on either eqn (37) or eqn (B4) given in Appendix B. We do the former by the method of Runge–Kutta combined with Adams–Bashforth multi-step. The biomass  $m(T, t)$  is given by eqn (35) as a function of  $A$  and  $S$ .

As for the nutrient-deficient model, we consider the case of semi-infinite domain where the nutrient concentration is kept constant as  $A_-$  at  $x_0 = 0$ , the substrate concentration remains to be  $S^+$  at  $x = \infty$  and the initial biomass concentration is  $m_0$  for the whole domain. In the following examples,  $A_- = 1.0$ ,  $S^+ = 1.0$ ,  $R_f = 1.5$ ,  $\gamma = 2.0$ ,  $m_0 = 0.2$ ,  $b = 0.5$ ,  $Y = 0.5$ , and  $q_0 = 0.3$  unless stated otherwise. As before,  $\langle n \rangle = 0.3$ ,  $\sigma_n^2 = 0.09$  and  $\lambda_n = 1.0$ .

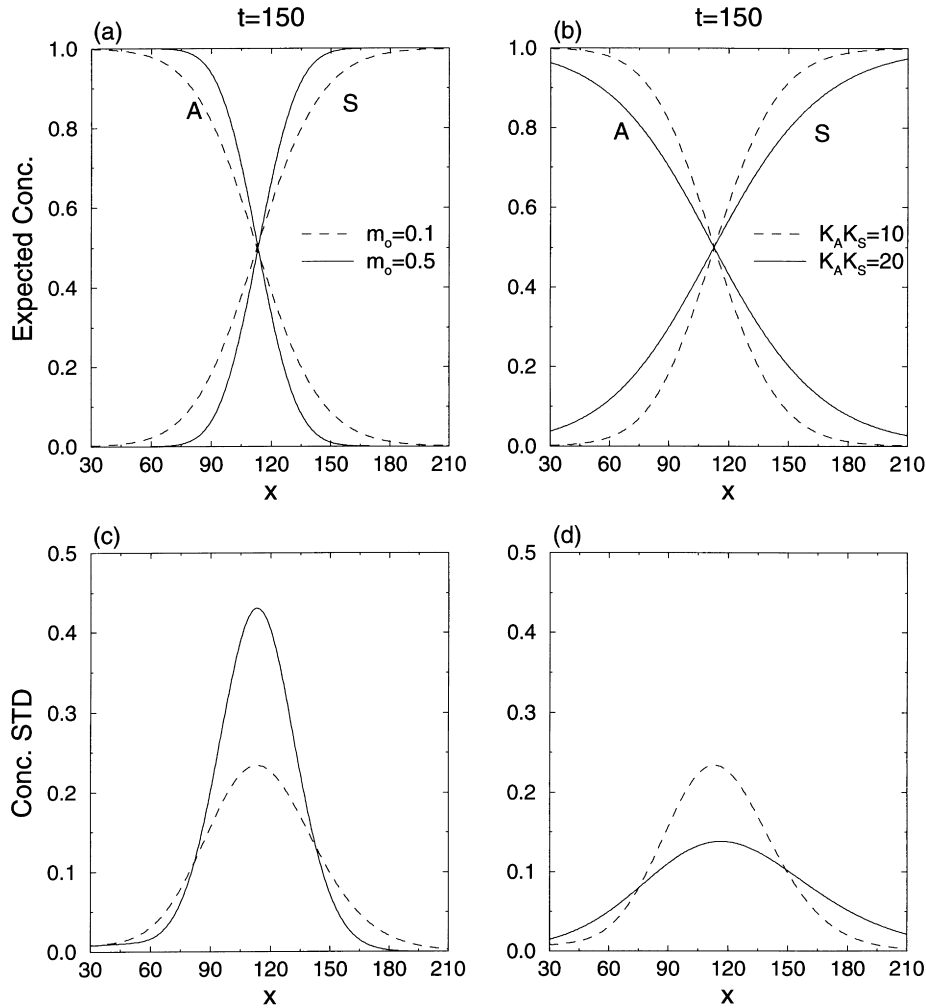


**Fig. 4.** Expected values and standard deviations of nutrient and substrate concentrations at  $t = 150$  for different geochemical and biological parameters: (a) and (c)  $m_0 = 0.1$  and  $0.5$ ; (b) and (d)  $K_A K_S = 10$  and  $20$ . (The nutrient-deficient model.)

Fig. 6 compares the general two component model with the nutrient deficient model for the case of homogeneous media ( $\sigma_n^2 = 0$ ). The objective is to investigate under what conditions the nutrient-deficient model gives a good approximation compared to the more general two component model. Fig. 6(a,b) shows the nutrient and substrate concentration profiles as functions of  $x - c_0vt$  for the cases of  $K_A = K_S = 1$  and  $K_A = K_S = 2$ , respectively. Fig. 6(c,d) show the corresponding biomass profiles. It is seen that the profiles of  $A$  and  $S$  are less steep (more dispersive) when predicted with the general two component model than with the nutrient-deficient model, and that the relative difference between these two models decreases with the increase of  $K_A$  and  $K_S$ . The latter observation is consistent with our expectation that the general two component model reduces to the nutrient-deficient model when  $(K_A, K_S)$  are large compared to  $(A_-, S^+)$ . The biomass concentration has a lower peak value and covers a larger area for larger  $(K_A, K_S)$ . It tends to the nutrient-deficient limit of constant biomass as  $(K_A, K_S)$  increases.

Fig. 7 shows the expected values of nutrient, substrate and biomass concentrations and their standard deviations for the case of random porosity ( $\sigma_n^2 = 0.09$ ). In this example,  $K_A = K_S = 2.0$ . For reference, the quantities for the homogeneous case are also presented. As in the nutrient-deficient model, the effect of heterogeneity on nutrient and substrate concentrations is to induce dispersive behaviors on their fronts (Fig. 7(a)), and the uncertainty as reflected in the standard deviation peaks at the center of the fronts (Fig. 7(c)). The heterogeneity also renders the biomass concentration a dispersive behavior, i.e. having a lower peak and covering a larger area compared to the homogeneous case (Fig. 7(b)). The standard deviation of biomass is largest at the center of the concentration profile (Fig. 7(d)). Though not shown, the dispersive behaviors become more apparent as the variance and correlation scale of porosity increase, as in the nutrient-deficient model.

Fig. 8 compares the total substrate removal and its rate for the nutrient-deficient model and the general two component model. The comparison is for the same case as in Fig.

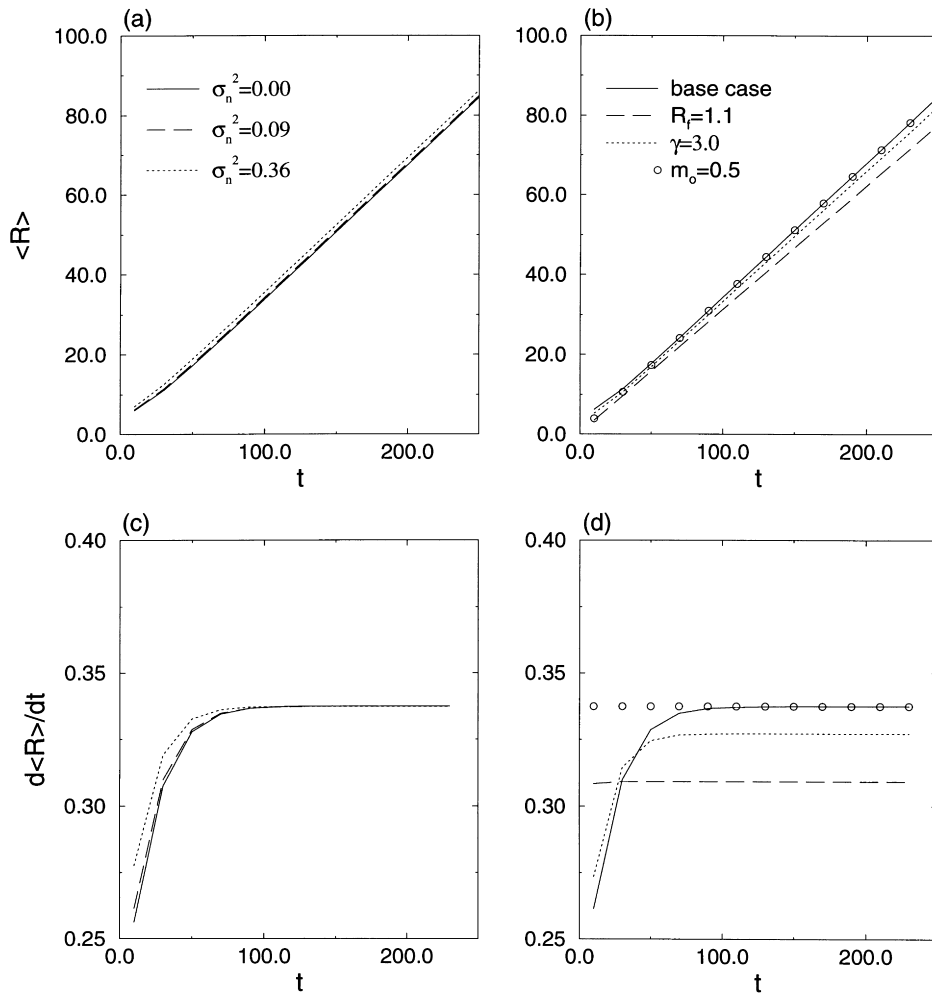


**Fig. 5.** Expected total substrate removal and its rate as functions of time: (a) and (c) for one homogeneous and two heterogeneous cases; (b) and (d) for various biological and geochemical parameters. (The nutrient-deficient model.)

7 where  $\sigma_n^2 = 0.09$  and  $K_A = K_S = 2.0$ . It is seen that the substrate removal and its rate for the general two component model are almost identical to their counterparts predicted by the nutrient-deficient model. Therefore, the degradation rate can also be expressed by eqn (57). The effects of heterogeneity and other factors such as mean flux, biological and geochemical parameters on the degradation rate are the same as discussed earlier for the nutrient-deficient model.

#### 4 SUMMARY

In this study, we have considered a biodegradation system of three coupled equations: two reaction–advection equations for nutrient and pollutant concentrations and one rate equation for biomass. The system is approximated by two two component models in the case that the decay rate of biomass is larger than the growth rate. Based on analytical or semi-analytical solutions derived for homogeneous cases, we have discussed constant

speed traveling fronts in these two models and compared their profiles.

For a spatially random water velocity field, we have introduced travel time and study statistics of degradation fronts via representations in terms of the travel time probability density function (*pdf*) and the traveling front profiles. The travel time *pdf* does not vary with the nutrient and pollutant concentrations but only depends on the pore water velocity. The traveling front profiles are given analytically or semi-analytically as functions of the travel time. Hence, the problem of nonlinear transport by a random velocity is reduced to two subproblems: one being nonlinear transport by a known (unit) velocity, and the other being linear (advective) transport by a random velocity.

In the examples of one-dimensional, steady-state flow, the flux  $q$  is a deterministic constant because the recharge at the boundary is assumed to be known. Then the only source of randomness or spatial variability is porosity. In this case, the statistical moments of travel time are given exactly in terms of those of porosity. With the

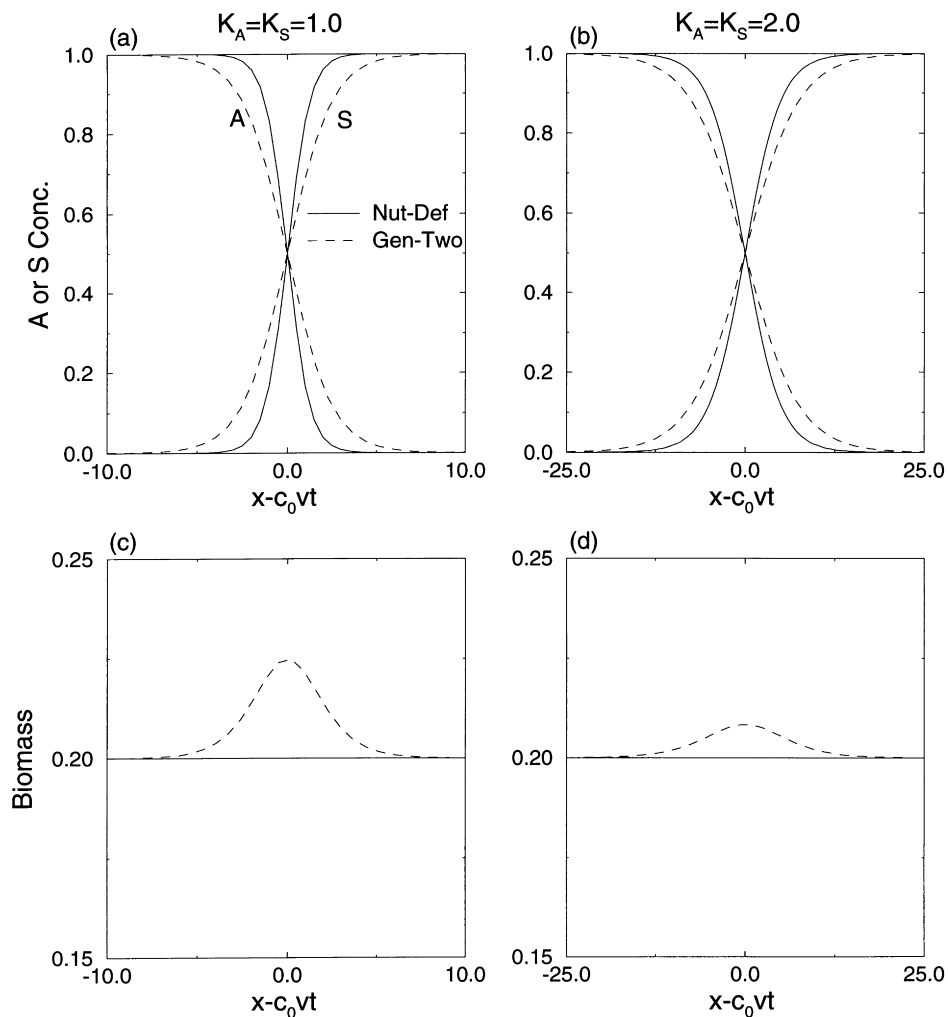


**Fig. 6.** Comparison of the general two component model and the nutrient-deficient model in homogeneous media: (a) and (c) for the case of  $K_A = K_S = 1.0$ ; (b) and (d) for the case of  $K_A = K_S = 2.0$ .

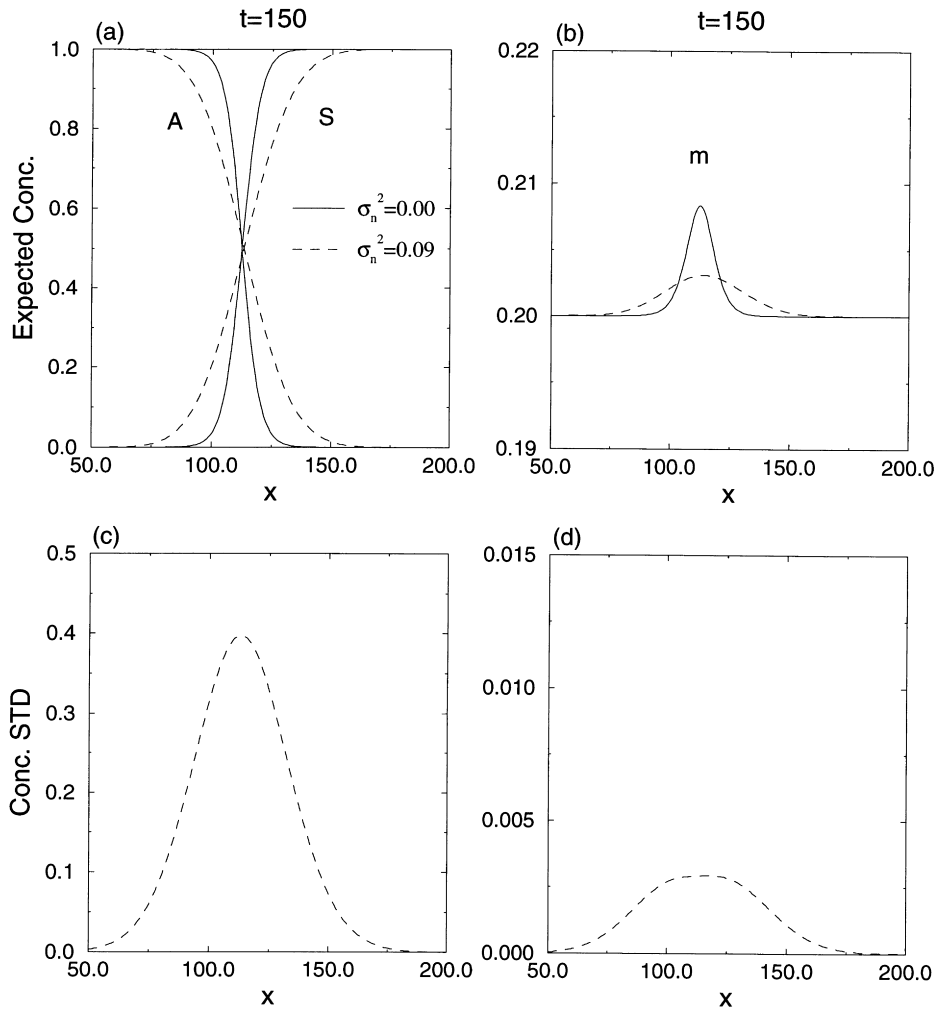


**Fig. 7.** Expected values and standard deviations of nutrient, substrate and biomass concentrations at  $t = 150$  for different porosity variances ( $\sigma_n^2 = 0$  and  $0.09$ ): (a) expected concentrations of nutrient and substrate; (b) expected biomass concentration; (c) standard deviation of nutrient and substrate concentrations ( $\sigma_A/A_- = \sigma_S/S^+$ ); and (d) standard deviation of biomass. (The general two component model.)

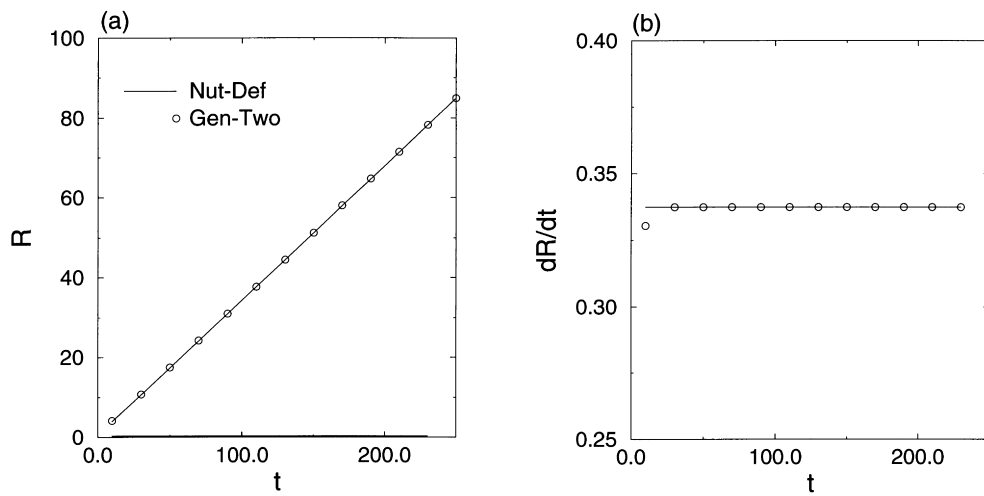


**Fig. 8.** Total substrate removal and its rate as functions of time for the case of  $\sigma_n^2 = 0.09$  and  $K_A = K_S = 2$ . (The general two component model.)

assumption that the travel time is lognormally distributed, the expected values and standard deviations of substrate, nutrient and biomass concentrations are evaluated by numerical integrations. The expected values of total substrate removal and its rate are evaluated similarly. It is found from these one-dimensional examples that medium heterogeneity induces dispersion and its effect generally increases with time and with the magnitude of spatial variability in porosity (as reflected in its variance and integral scale). The uncertainty in predicting the concentration profiles is largest at the center of the profiles and increases with the variability in porosity. It is found that the total substrate removal rate at late time is not affected by the presence of heterogeneity for the present model system.

The geochemical and biological parameters significantly impact the concentration prediction, the associated uncertainty, and the predicted biodegradation rate. The uncertainty and/or spatial variability in these parameters should be investigated in future studies.

## ACKNOWLEDGEMENTS

We wish to thank D. Holm and B. Travis at Los Alamos National Laboratory (LANL) for organizing the SIAM workshop on bioremediation in June of 1997 at LANL where our collaboration was initiated. The work was partially supported by NSF Grant DMS-9625680 (to J. Xin) and LANL LDRD Project #97528 (to D. Zhang). We would also like to thank the two anonymous reviewers for their constructive comments and suggestions.

## REFERENCES

- Borden, R. C. and Bedient, P. B. Transport of dissolved hydrocarbons influenced by oxygen-limited biodegradation. 1. Theoretical development. *Water Res. Research*, 1986, **22**, 1973–1982.
- Borden, R. C., Bedient, P. B., Lee, M. D., Ward, C. H. and Wilson, J. T. Transport of dissolved hydrocarbons influenced by oxygen-limited biodegradation. 2. Field application. *Water Res. Research*, 1986, **22**, 1983–1990.
- Chen, Y.-M., Abriola, L. M., Alvarez, P. J. J., Anid, P. J. and Timothy, M. V. Modeling transport and biodegradation of benzene and toluene in sandy aquifer material: Comparisons with experimental measurements. *Water Res. Research*, 1992, **28**, 1833–1847.
- Corapcioglu, M. Y. and Haridas, A. Microbial transport in soils and groundwater: A numerical model. *Adv. Water Resour.*, 1985, **8**, 188–200.
- Ginn, T. R., Simmons, C. S. and Wood, B. D. Stochastic-convective transport with nonlinear reaction: Biodegradation with microbial growth. *Water Res. Research*, 1995, **31**, 2689–2700.
- Hess, A., Hohener, P., Hunkeler, D. and Zeyer, J. Bioremediation of a diesel fuel contaminated aquifer: Simulation studies in laboratory aquifer columns. *J. Contam. Hydrol.*, 1996, **23**, 329–345.
- Hess, A., Hohener, P., Hunkeler, D. and Zeyer, J. Bioremediation of a diesel fuel contaminated aquifer: Simulation studies in laboratory aquifer columns. *J. Contam. Hydrol.*, 1995, **31**, 2689–2700.
- Kinzelbach, W., Schafer, W. and Herzer, J. Numerical modeling of nitrate and enhanced denitrification processes in aquifers. *Water Resour. Res.*, 1991, **27**, 1123–1135.
- MacQuarrie, K. T. B., Sudicky, E. A. and Frind, E. O. Simulation of biodegradable organic contaminants in groundwater: 1. Numerical formulation in principal directions. *Water Resour. Res.*, 1990, **26**, 207–222.
- Molz, F. J., Widdowson, M. A. and Benefield, L. D. Simulation of microbial growth dynamics coupled to nutrient and oxygen transport in porous media. *Water Res. Research*, 1986, **22**, 1207–1216.
- Odencrantz, J. E., Valocchi, A. J. & Rittmann, B. E., Modeling the interaction of sorption and biodegradation on transport in groundwater *in situ* bioremediation systems. In *Proc. 1993 Groundwater Modeling Conference*, ed Poeter, E. et al., Golden, CO, 1993.
- Oya, S. and Valocchi, A. J. Characterization of traveling waves and analytical estimation of pollutant removal in one-dimensional subsurface bioremediation modeling. *Water Resour. Res.*, 1997, **33**, 1117–1127.
- Sykes, J. F., Soyupak, S. and Farquhar, G. J. Modeling of leachate organic migration and attenuation in ground waters below sanitary landfills. *Water Res. Research*, 1982, **18**, 135–145.
- Widdowson, M. A., Molz, F. J. and Benefield, L. D. A numerical transport model of oxygen- and nitrate-based respiration linked to substrate and nutrient availability in porous media. *Water Res. Research*, 1988, **24**, 1553–1565.
- Murray, R. & Xin, J., Existence of traveling waves in a biodegradation system. *SIAM J. Math. Analysis*, 1998, in press.
- Xin, J. & Hyman, J., Relaxation, stability, and oscillation of bioremediation fronts. Preprint, 1997.
- Wood, B. D., Dawson, C. N., Szecsody, J. E. and Streile, G. P. Modeling contaminant transport and biodegradation in a layered porous media system. *Water Res. Research*, 1994, **30**, 1833–1845.
- Miralles-Wilhelm, F., Gelhar, L. W. and Kapoor, V. Stochastic analysis of oxygen-limited biodegradation in three-dimensionally heterogeneous aquifers. *Water Resour. Res.*, 1997, **33**, 1251–1263.
- Zhang, D. & Tchelepi, H., Stochastic analysis of immiscible two-phase flow in heterogeneous media. Submitted to *SPE J.*, 1997.

## APPENDIX A THE NUTRIENT-DEFICIENT MODEL

To derive the formulas eqns (28)–(30), we substitute the form of traveling fronts in eqns (26) and (27) to get:

$$-c_0 \frac{du_0}{d\xi} + \frac{dw_0}{d\xi} = 0, \quad (\text{A1})$$

$$\begin{aligned} -c_0 \frac{dw_0}{d\xi} + \left( -R_f^{-1} \frac{du_0}{d\xi} + (1 + R_f^{-1}) \frac{dw_0}{d\xi} \right) \\ = \tilde{\gamma}(u_0 - w_0)(u_0 - R_f w_0). \end{aligned} \quad (\text{A2})$$

Integrating eqn (A1) in  $\xi$  and applying the boundary conditions at infinity yields eqns (28) and (29). Plugging eqn

(29) into eqn (A2), we get:

$$\begin{aligned} & -c_0 \frac{dw_0}{d\xi} + (1 + R_f^{-1}) \frac{dw_0}{d\xi} - \frac{1}{R_f} c_0^{-1} \frac{dw_0}{d\xi} \\ &= \tilde{\gamma} \left( \left( \frac{1}{c_0} - 1 \right) w_0 + \left( \frac{1 - c_0}{c_0} \right) A_- \right) \left( \left( \frac{1}{c_0} - R_f \right) w_0 \right. \\ & \left. + \left( \frac{1 - c_0}{c_0} \right) A_- \right), \end{aligned}$$

or:

$$\begin{aligned} & \left( -c_0 + (1 + R_f^{-1}) - \frac{1}{R_f} c_0^{-1} \right) \frac{dw_0}{d\xi} = \tilde{\gamma} \left( \frac{1}{c_0} - 1 \right) \\ & \times \left( \frac{1}{c_0} - R_f \right) (w_0 + A_-) \left( w_0 + \frac{1 - c_0}{1 - R_f c_0} A_- \right). \end{aligned}$$

Using eqn (28), the above equality becomes:

$$\frac{dw_0}{d\xi} = - \frac{\tilde{\gamma} R_f (\gamma R_f S^+ + A_-)}{(\gamma S^+ + A_-)} (w_0 - \gamma S^+) (w_0 + A_-). \quad (\text{A3})$$

Recall that the ODE ( $\alpha > 0$ ,  $a_1 < a_2$ ):

$$\frac{dw}{d\xi} = -\alpha(w - a_1)(w - a_2)$$

under the boundary conditions  $w(-\infty) = a_1$ ,  $w(+\infty) = a_2$  has unique solution:

$$w = \frac{1}{2}(a_1 - a_2) \tanh\left(\frac{\alpha}{2}(a_1 - a_2)\xi\right) + \frac{a_1 + a_2}{2}$$

up to a constant translate in  $\xi$ . The formula eqn (30) follows.

We observe that the wave profiles are strictly increasing in  $\xi$ :

$$\frac{du_0}{d\xi} > 0, \quad \frac{dw_0}{d\xi} > 0, \quad \forall \xi. \quad (\text{A4})$$

In view of eqns (24) and (29), we have from eqn (A4):

$$\frac{dA_0}{d\xi} < 0, \quad \frac{dS_0}{d\xi} > 0, \quad \forall \xi. \quad (\text{A5})$$

## APPENDIX B THE GENERAL TWO COMPONENT MODEL

Thus eqn (37) gives  $w_0 = w_0(\xi)$  with  $w_0(0) = (\gamma S^+ - A_-)/2$  as:

$$\begin{aligned} & \int_{(\gamma S^+ - A_-)/2}^{w_0} \frac{G(w)}{(w - \gamma S^+)(w + A_-)} dw = \\ & - \frac{\tilde{\gamma} R_f (R_f S^+ + A_-)}{(\gamma S^+ + A_-)} \xi. \end{aligned} \quad (\text{B1})$$

With eqn (B1) in place of eqn (30), we have found the traveling front formula in general.

The integral in eqn (B1) is available in closed form. Consider the integral:

$$\int \frac{\alpha x^2 + \beta x + \gamma'}{(x - a)(x - b')} dx,$$

which is equal to:

$$\alpha x + \int \frac{cx + d}{(x - a)(x - b')} dx, \quad (\text{B2})$$

where:

$$c = \alpha(a + b') + \beta, \quad d = \gamma' - \alpha ab'. \quad (\text{B3})$$

The second term of eqn (B2) is equal to:

$$(a - b')^{-1} [(ac + d) \log|x - a| - (b'c + d) \log|x - b'|].$$

Combining the above, we have the formula for the profile of  $w_0$ :

$$\begin{aligned} & .\alpha w_0 + (a - b')^{-1} [(ac + d) \log|w_0 - a| \\ & - (b'c + d) \log|w_0 - b'|] = \alpha w \\ & + (a - b')^{-1} [(ac + d) \log|w - a| - (b'c + d) \\ & \times \log|w - b'|] \Big|_{w=(\gamma S^+ - A_-)/2} - \frac{\tilde{\gamma} R_f (\gamma R_f S^+ + A_-)}{(\gamma S^+ + A_-)} \xi, \end{aligned} \quad (\text{B4})$$

where  $a = \gamma S^+$ ,  $b' = -A_-$ , and:

$$\alpha = -(1 - b^{-1}Y) \frac{S^+ A_-}{K_A K_S (\gamma S^+ + A_-)^2}, \quad (\text{B5})$$

$$\begin{aligned} \beta &= \frac{S^+}{K_S (S^+ + A_-)} - \frac{A_-}{K_A (S^+ + A_-)} \\ & - (1 - b^{-1}Y) \frac{S^+ A_- (A_- - S^+)}{K_S K_A (S^+ + A_-)^2}, \end{aligned} \quad (\text{B6})$$

$$\begin{aligned} \gamma' &= 1 + (K_S^{-1} + \gamma K_A^{-1}) \frac{S^+ A_-}{(\gamma S^+ + A_-)} \\ & + \gamma (1 - b^{-1}Y) \frac{(S^+ A_-)^2}{K_S K_A (\gamma S^+ + A_-)^2}. \end{aligned} \quad (\text{B7})$$